Numerical Analysis of Surface Acoustic Wave Driven Carriers Transport in GaAs/AlGaAs Quantum Well

Pang Ziliang

May 10, 2023

Numerical analysis of surface acoustic wave driven carriers transport in GaAs/AlGaAs quantum well

Ziliang Pang

Abstract. The surface acoustic waves (SAWS) with a strong enough piezoelectric field can capture and transport electrons and holes. The presence of the surface acoustic waves and their photo-generated carriers transport properties in the GaAs/AlGaAs quantum well (QW) is a potential scheme to achieve single photon sources and single photon detectors. In this work, we numerically solve the system of coupled Schrödinger and Poisson equations and the carriers radiative lifetime. A finite difference method (FDM) of two dimensional was developed as a conventional approach to the theoretical understandings of the presence in the QW through Python programs. The features of carriers radiative lifetime are discussed as functions of the SAW wavelengths and SAW amplitudes. The spatial separation and radiative lifetime extending of the electrons and holes in SAW-driven QW could be explained by the method.

Keywords: surface acoustic waves, quantum well, Single-photon devices, python.

1 Introduction

Future rising demand for quantum computing and information can be achieved using photonic qubits.[1–6] Photons are the quantum objects of encode, communicate, manipulate, and measure information. Many quantum phenomena are experimentally observed in semiconductor low-dimensional devices.[7–9] There is progressive interest in a two-dimensional electron gas (2DEG) because of the widely investigation of the GaAs-based high-electron-mobility-transistor (HEMT) system, and it becomes the most popular system for various physics effects such as ballistic electron transport,[9] Coulomb blockade,[10] and spin read-out.[11] The AlGaAs/GaAs heterostructures system is a common GaAs-based heterostructures for obtaining a 2DEG.[12–14] A scheme that can be used for prolonging the lifetimes of the optical excitations was proposed by Rocke.[15] The long-range transport of the optical excitations has been demonstrated by J. Rudolph.[16] It is a promising method to achieve single photon sources and single photon detectors.[17–22] This makes use of the fact that, in a semiconductor piezoelectric material, the electrons and holes are separated by SAWs that are accompanied with periodical potential as shown in Fig. 1(a).[16,23–25] There has been an extensive study in order to develope SAW-driven single photons devices.[26] Almost all the research of SAW-driven single photons devices has been carried out on the AlGaAs/GaAs heterostructures systems,[27–34] because GaAs and AlGaAs are piezoelectric. There has been an extensive study in order to develope SAW-driven single photons devices that use the AlGaAs/GaAs heterostructures systems as shown in Fig. 1(b). Here, we present a theoretical framework for SAW-driven 2DEG and analysis the key contributors to radiative lifetime of the 2DEG in AlGaAs/GaAs heterostructures QW.

(a)

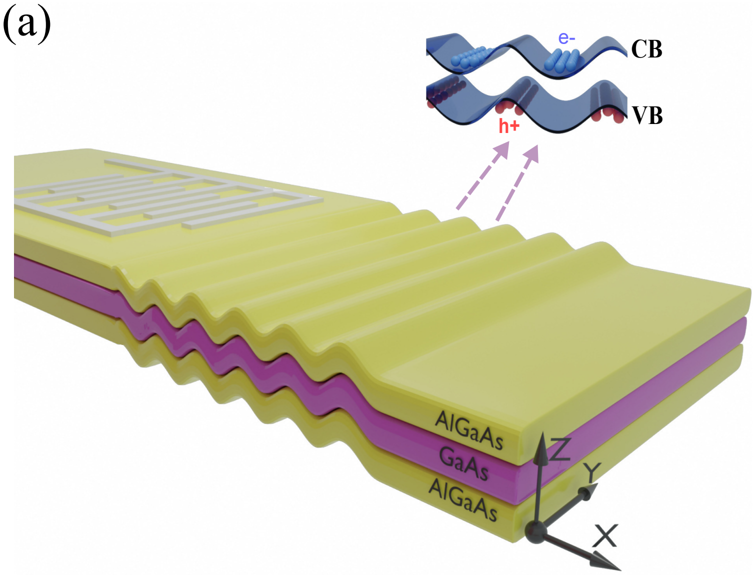

(b)

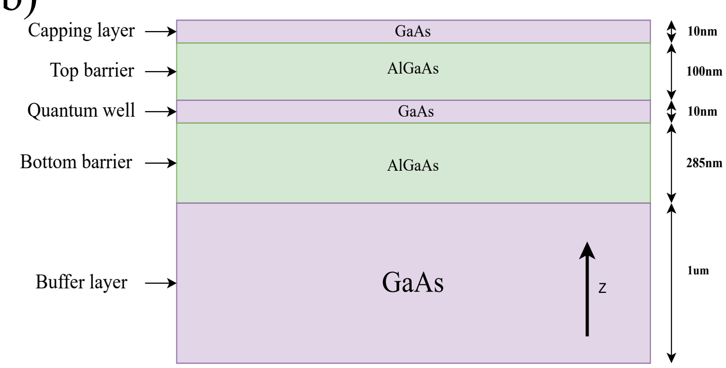

Fig 1 (a) The three-dimensional(3D) schematic view shows the concept and structure of the SAW-driven 2DEG devices. (b) Schematic diagram of the AlGaAs/GaAs heterostructures.

2 Theoretical model

2.1 The one-dimensional (1D) model for a AlGaAs/GaAs QW

The 1D model is achieved by the known self-consistent Schrödinger-Poisson equation solving scheme.[35–37] The single-particle time-independent Schrodinger equation can be given as:

$$-\frac{\hbar^2}{2m^*}\frac{\partial^2}{\partial z^2}\psi(z) + V(z)\psi(z) = E\psi(z), \tag{1}$$

where m^* is the particle mass, V is an arbitrary confining barrier potential, and E is the energy of state. All the physical constants of the models are summarized in Table 1. By applying the Finite Difference Method (FDM) to a number of spatial locations, the Schrodinger equation can be discretised as:

$$-\frac{\hbar^2}{2m^*}\left[\frac{\psi(z+\delta z) - 2\psi(z) + \psi(z-\delta z)}{(\delta z)^2}\right] + V(z)\psi(z) = E\psi(z). \tag{2}$$

The matrix form of the discretised schrodinger equation, can be represented by:

$$\mathrm{H}\boldsymbol{\psi} = E\boldsymbol{\psi} \tag{3}$$

The equation can be solved to locate the eigenvalues and wave functions. The space-charge effects of charge carriers, obtained by solving Poisson's equation, can be expressed by an additional potential:

$$\mathrm{V}(z) = \mathrm{V}_{CB}(z) + \mathrm{V}_{\rho}(z) \tag{4}$$

where V_{CB} is the band-edge potential and V_ρ is the potential of the charge. The new value of potential can be used to solve for new charge distribution. We ought to repeat the process over and over again until the results of the solution converge.

2.2 The two-dimensional (2D) model of the 2DEG in a QW system

The potential that generated by SAW can controls carriers capture and recombination in xy-plane of the GaAs.[38,39] Inspired by the envelope function model of Bretagnon in [40], we can simulate the carriers radiative lifetime by solving the Schrodinger equation. The single-particle time-independent Schrodinger equation in the xy-plane can be given as:

$$-\frac{\hbar^2}{2m^*}\left(\frac{\partial^2\psi}{\partial x^2}+\frac{\partial^2\psi}{\partial y^2}\right)+V(x,y)\psi=E\psi. \tag{5}$$

The radiative lifetime τ_{rad} of excitons is given by:

$$\tau_{rad}=\frac{2\pi\varepsilon_0 m_e c^3}{ne^2\omega_{cv}^2 f_{osc}}, \tag{6}$$

where f_{osc} is excitonic oscillator strength that is proportional to the square of the overlap integral between wave functions of electron and hole $f_{osc}=\left|\int f_e(z)f_h(z)dz\right|^2$.[41,42]

3 Simulation Results and discussion

3.1 Simulation of 2DEG characterization in the semiconductor thin film growth direction

We start from 1D simulation of GaAs/AlGaAs heterostructures, as shown in Fig,1b. The domain length is defined as 50 nm, and a 0.5 Å sampling period was used. Here, the Al content of $Al_{0.33}Ga_{0.67}As$ layers gives the depth of the potential well of V_0 = 286 meV.[35] A 10nm GaAs

Table 1 physical constants of the model

Electron effective mass(GaAs)	0.067
Hole effective mass(GaAs)	0.45
Electron Mass	$9.1093826 \times 10^{-31} kg$
Electron Charge	$1.602176 \times 10^{-19} C$
$\hbar$	$1.054588757 \times 10^{-34} Js$
Boltzmann constant	$1.3806504 \times 10^{-23} J/K$
Vacuum permittivity	$8.8541878176 \times 10^{-12} F/m$
relative permittivity(GaAs)	13.1

space-layer is embedded in two layers of $Al_{0.33}Ga_{0.67}As$ of 100 nm and 285 nm thick at a temperature $T = 300K$. The total number N of photo-generated electrons density in the quantum well is around $8 \times 10^{17} cm^{-3}$.[43] A 10 nm GaAs capping layer is designed to prevent the oxidation of the Al atoms in the $Al_{0.33}Ga_{0.67}As$ layer. In the QW, the electron wave functions are calculated by solving the self-consistent Schrödinger-Poisson equation.

The self-consistent solution of Schrödinger-Poisson equations of the system is depicted in Fig.3. The Python program uses $numpy$ and $matplotlib$ libraries to achieve calculations and present graphs. Figure 2(a) shows the result of adding the potential of charge distribution. The two confined eigenstates of the GaAs quantum well is depicted in Figure 2(b). Figure 2(c) shows the areal charge density along the growth axis for the 10nm GaAs well. The potential due to the electron distribution is illustrated in Fig.3(d). As shown in Fig. 2(b), the photo-generated free electrons are confined to a 2D plane by the strong potential barriers, which is known as a 2DEG.

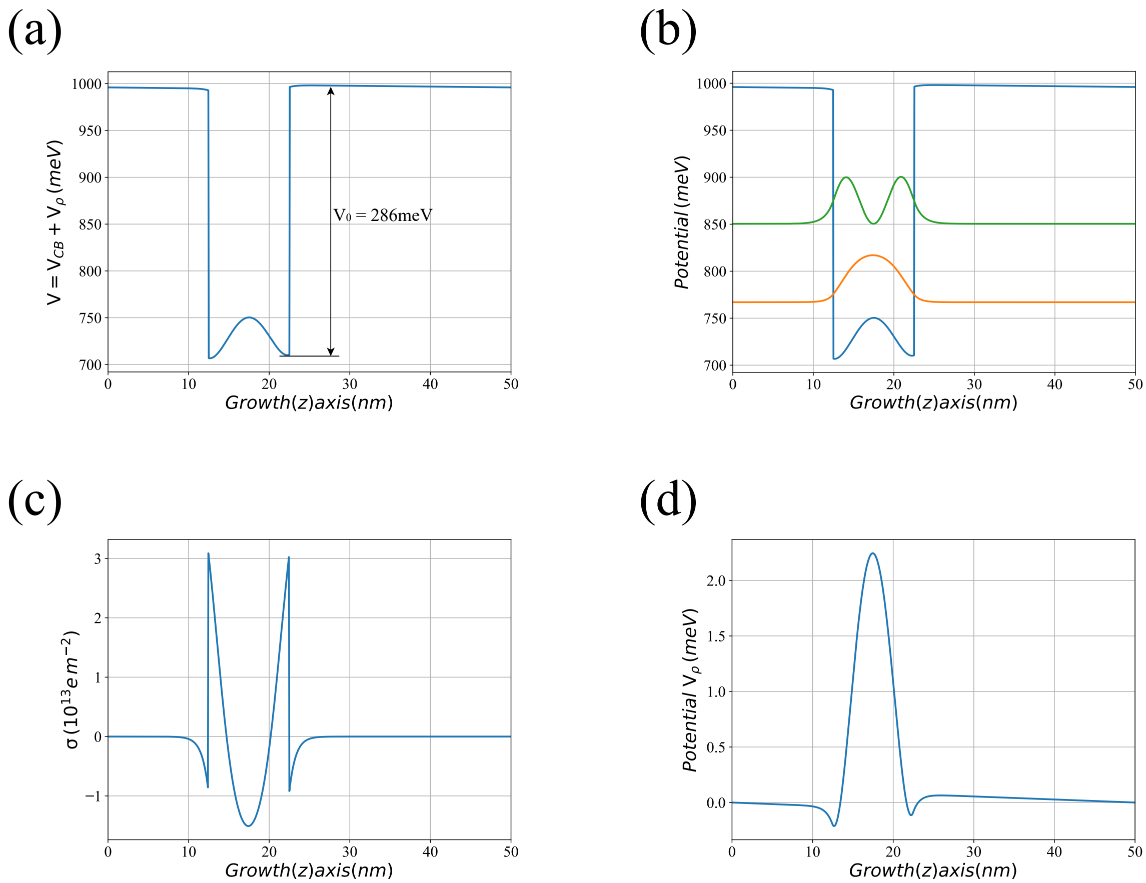

Fig 2 (a)The sum of the V_{CB} and Poisson's potential V_ρ for the GaAs quantum well,(b)The two confined eigenstates of the GaAs quantum well,(c)Areal charge density σ for the GaAs quantum well,(d)The potential due to the electron distribution.

3.2 Simulation of SAW-driven photo-generated carriers radiative lifetime in xy-plane

We model a periodical potential field of SAW in the 2DEG of the GaAs/ $Al_{0.33}Ga_{0.67}As$ heterostructure in xy-plane, as shown in Fig. 3. The thin film heterostructure is the same as that in the 1D simulation.The thin film heterostructure is the same as that in the 1D simulation. In the model, we assume that SAW potential is a sine wave in the x direction and decays exponentially in the y direction, as shown in Fig. 3(a) and Fig. 3(b). The eigenfunction of the potential field can be obtained by solving Eq(5). The electron probability density for the SAW potential field(Fig. 3) is shown in Fig. 3(c).

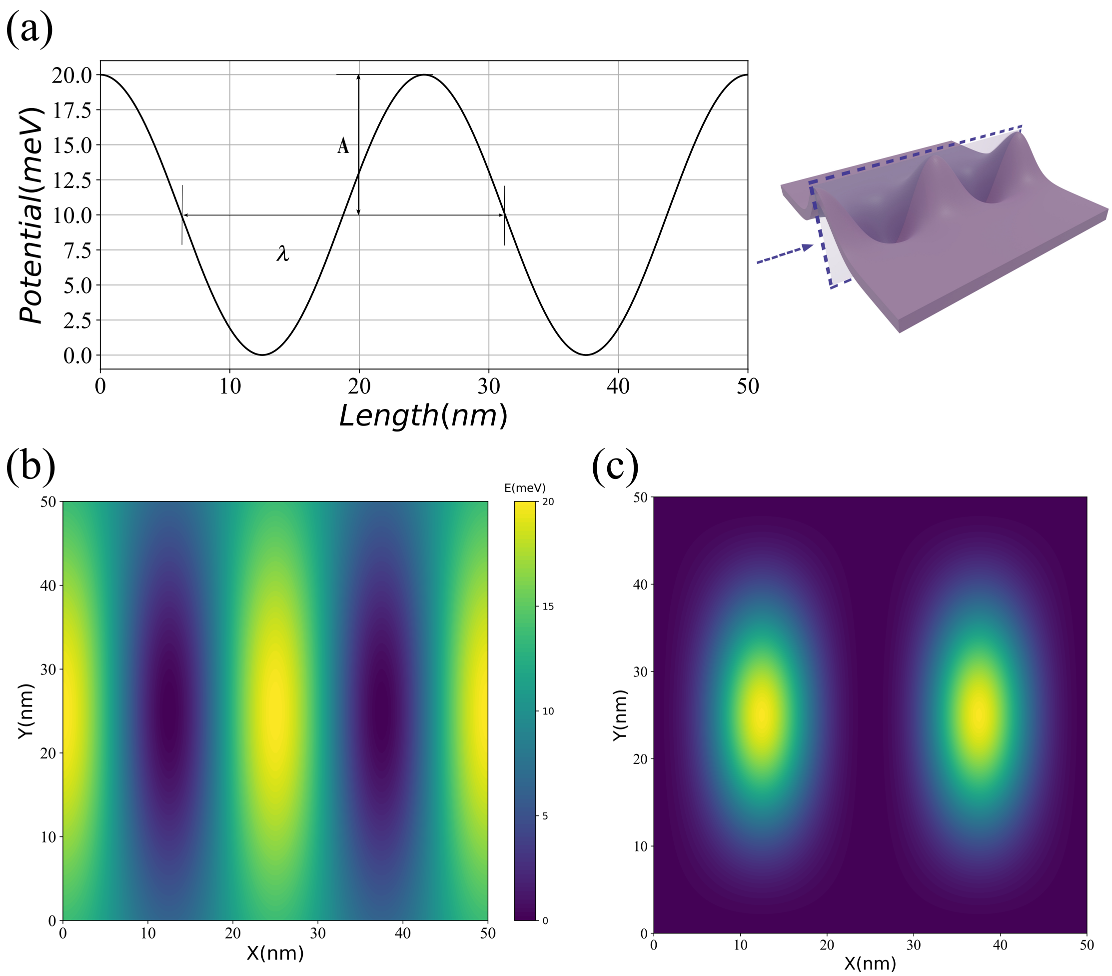

Fig 3 (a) A schematic diagram of the SAW potential in the x direction. (b) 2D SAW potential map in the QW of the GaAs heterostructure. (c) Eigenfunction calculated in the SAW potential.

The interband transition of the QW heterostructures usually occurs between the first electron QW state and the first heavy hole QW state.[42] The interband oscillator strength and photogenerated carriers radiative lifetime is proportional to the square of the overlap integral between the electron and hole probability density functions.[40,42] In fig.4(a), the 1D electron and hole probability density functions with 1D SAW potential as been simulated using python program.[41] The 3-dimensional schematic diagram in Fig.4(b) shows the 2D electron and hole probability density functions with 2D SAW potential. This 2D model is more realistic than the previous 1D SAW potential model.[41] The SAW amplitude(A) and wavelength length (λ) can be considered separately as illustrated in Fig.3(a).

(a) (b)

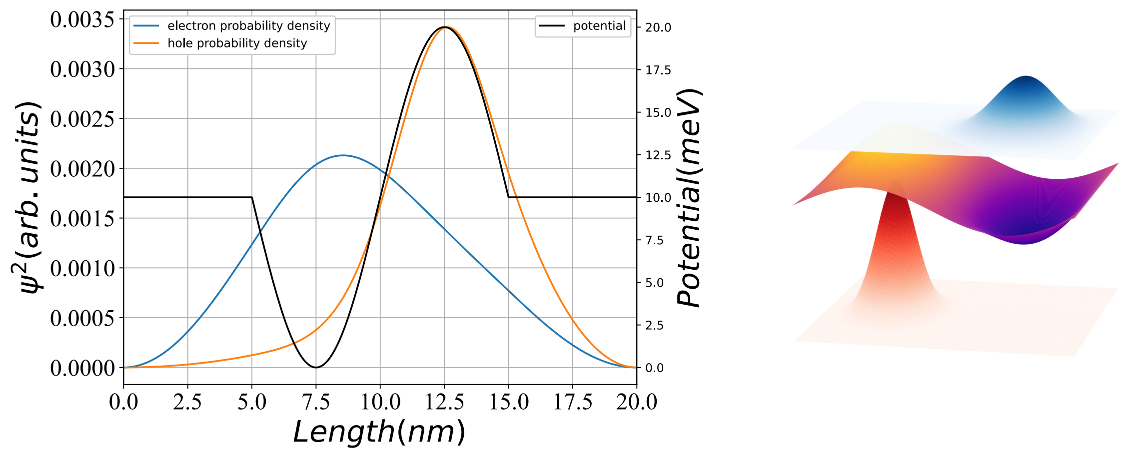

Fig 4 (a) the 1D Electron and hole probability densities with the SAW potential. (b) The 3D schematic view of the 2D Electron and hole probability densities with the SAW potential.

Figure.5 shows the normalized square of the overlap integral between the 2D electron and hole probability density functions as a function of the SAW amplitude in a range of 10–48 meV, selectively for λ= 20, 30, and 40 nm. Figure.6 shows the normalized corresponding radiative lifetimes $\tau_{\text{rad}} = A/\left|\int f_e(z)f_h(z)\right|^2$ as a function of SAW amplitude in units of meV with different SAW wavelength length from 20 to 24 nm, where A is the only adjustable parameter.

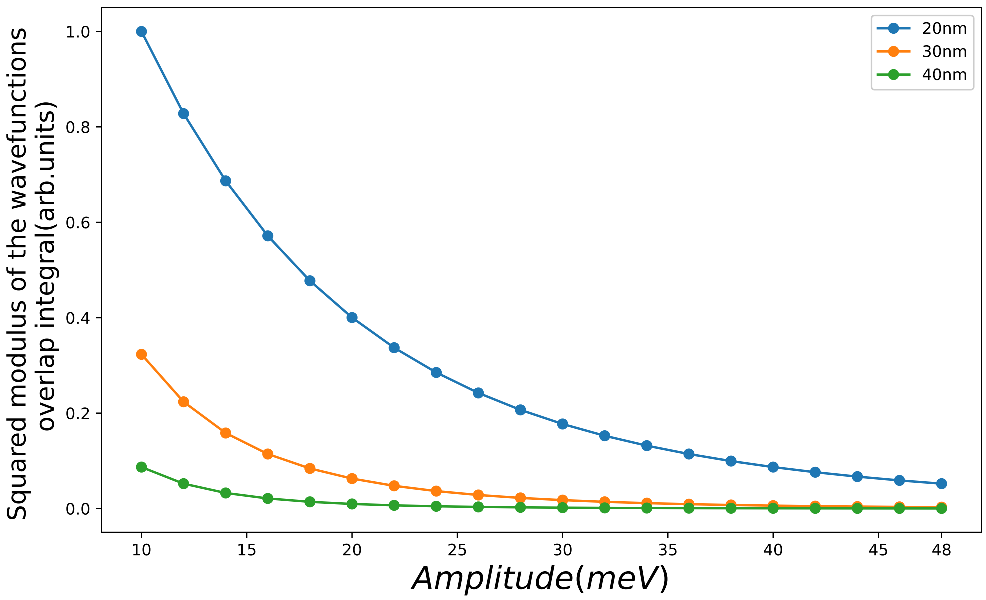

Fig 5 the square of the overlap integral between the 2D electron and hole probability density functions as a function of SAW amplitude from 10 to 48 meV at different SAW wavelength length λ= 20, 30, and 40 nm.

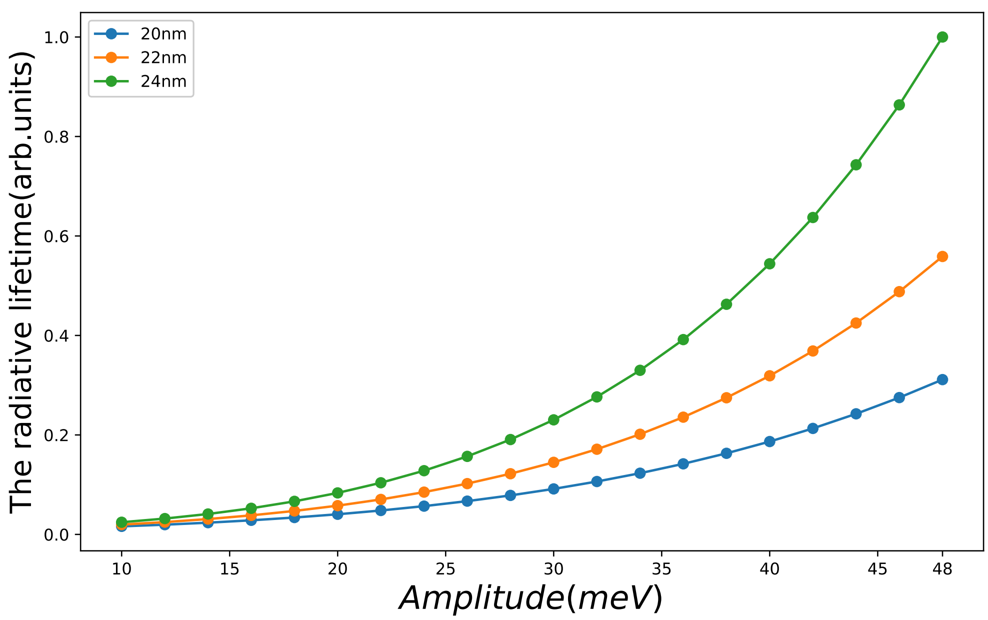

Fig 6 the radiative lifetimes as a function of SAW amplitude from 10 to 48 meV at different SAW wavelength length λ= 20, 22, 24 nm.

To improve the radiative lifetimes of the SAW-driven photo-generated carriers in the QW, a further attempt at enhancement of the SAW amplitude and wavelength is still important, by using the simulations. In the simulation of SAW-driven photo-generated carriers in the QW, we verify the possibility of extending the radiative lifetimes of the photo-generated carriers, and also explain why the electrons and holes photogenerated can be transported in a surface acoustic wave.[15]

4 Conclusion

In this study, we developed a newly method to numerically analyze the extending of photo-generated carrier lifetimes in SAW-driven QW devices. We present the results of different SAW wavelengths and SAW amplitudes. A 1D self-consistent Schrödinger-Poisson equation solver in z-axis and a 2D FDM solver with a 2D potential of SAW potential well were developed in Python. With these solvers, it is possible to produce an accurate model and to optimise complex SAW-driven QW devices. These numerical simulations show great potential in terms of the device design and optimisation, and pave the way for a high-quality SAW-driven QW Single photon devices.

Data, Materials, and Code Availability

The raw data of the simulations can be downloaded from [https://doi.org/10.5281/zenodo.7655457].

References

1 E. Knill, R. Laflamme, and G. J. Milburn, "A scheme for efficient quantum computation with linear optics," *Nature* **409**, 46–52 (2001).

2 J. Chen, J. B. Altepeter, M. Medic, *et al.*, "Demonstration of a quantum controlled-not gate in the telecommunications band," *Phys. Rev. Lett.* **100**, 133603 (2008).

3 M. Halder, A. Beveratos, N. Gisin, *et al.*, "Entangling independent photons by time measurement," *Nature Physics* **3**, 692–695 (2007).

4 C. Clausen, I. Usmani, F. Bussières, *et al.*, "Quantum storage of photonic entanglement in a crystal," *Nature* **469**, 508–511 (2010).

5 A. Wallraff, D. I. Schuster, A. Blais, *et al.*, "Circuit quantum electrodynamics: Coherent coupling of a single photon to a cooper pair box," *Physics* (2004).

6 M. Hofheinz, H. Wang, M. Ansmann, *et al.*, "Synthesizing arbitrary quantum states in a superconducting resonator," *Nature* **459**(7246), 546–9 (2009).

7 R. B. Laughlin, "Quantized hall conductivity in two dimensions," *Phys. Rev. B* **23**, 5632–5633 (1981).

8 Stotz, A. H. James, Hey, *et al.*, "Coherent spin transport through dynamic quantum dots.," *Nature Materials* (2005).

9 K. J. Thomas, M. Y. Simmons, J. T. Nicholls, *et al.*, "Ballistic transport in one-dimensional constrictions formed in deep two-dimensional electron gases," *Applied Physics Letters* **67**, 109–111 (1995).

10 C. Livermore, C. Crouch, R. Westervelt, *et al.*, "The coulomb blockade in coupled quantum dots," *Science* **274**(5291), 1332–1335 (1996).

11 R. Hanson, L. H. W. van Beveren, I. T. Vink, *et al.*, "Single-shot readout of electron spin states in a quantum dot using spin-dependent tunnel rates," *Phys. Rev. Lett.* **94**, 196802 (2005).

12 H. Hou, *Low-dimensional electron transport and surface acoustic waves in GaAs and ZnO heterostructures*. PhD thesis, University of Cambridge (2018).

13 F. Alsina, P. Santos, R. Hey, *et al.*, "Dynamic carrier distribution in quantum wells modulated by surface acoustic waves," *Physical Review B* **64**(4), 041304 (2001).

14 V. Talyanskii, J. Stotz, and P. Santos, "An acoustoelectric single photon detector," *Semiconductor science and technology* **22**(3), 209 (2007).

15 C. Rocke, S. Zimmermann, A. Wixforth, *et al.*, "Acoustically driven storage of light in a quantum well," *Phys. Rev. Lett.* **78**, 4099–4102 (1997).

16 J. Rudolph, R. Hey, and P. Santos, "Exciton transport by surface acoustic waves," *Superlattices and Microstructures* **41**(5-6), 293–296 (2007).

17 Y. Chung, H. Hou, S.-K. Son, *et al.*, "Quantized charge transport driven by a surface acoustic wave in induced unipolar and bipolar junctions," *Physical Review B* **100**(24), 245401 (2019).

18 S. Jiao, P. D. Batista, K. Biermann, *et al.*, "Efficient photon detectors using surface acoustic waves," *Physica E: Low-dimensional Systems and Nanostructures* **42**(10), 2857–2861 (2010).

19 T. Sogawa, P. Santos, S. Zhang, *et al.*, "Transport and lifetime enhancement of photoexcited spins in gaas by surface acoustic waves," *Physical review letters* **87**(27), 276601 (2001).

20 G. De Simoni, V. Piazza, L. Sorba, *et al.*, "Acoustoelectric luminescence from a field-effect n-i-p lateral junction," *Applied Physics Letters* **94**(12), 121103 (2009).

21 J. Gell, P. Atkinson, S. Bremner, *et al.*, "Surface-acoustic-wave-driven luminescence from a lateral p-n junction," *Applied physics letters* **89**(24), 243505 (2006).

22 B. Dong, A. Afanasev, R. Johnson, *et al.*, "Enhancement of photoemission on p-type gaas using surface acoustic waves," *Sensors* **20**(8), 2419 (2020).

23 F. Alsina, P. Santos, and R. Hey, "Spatial-dispersion-induced acoustic anisotropy in semiconductor structures," *Physical Review B* **65**(19), 193301 (2002).

24 F. Alsina, J. Stotz, R. Hey, *et al.*, "Acoustically induced potential dots in gaas quantum wells," *Solid state communications* **129**(7), 453–457 (2004).

25 S. Jiao, P. Batista, K. Biermann, *et al.*, "Electrical detection of ambipolar acoustic carrier transport by surface acoustic waves," *Journal of Applied Physics* **106**(5), 053708 (2009).

26 A. Rubino, *SAW-driven single-photon sources and photon detectors fabricated on an undoped GaAs/AlGaAs quantum well*. PhD thesis, Department of Physics University of Cambridge (2019).

27 V. M. Yakovenko, "Novel method for photovoltaic energy conversion using surface acoustic waves in piezoelectric semiconductors," *Physica B: Condensed Matter* **407**(11), 1969–1972 (2012).

28 V. Talyanskii, V. Kachkanov, and P. Santos, "Fidelity of the charge transport by surface acoustic waves in a gaas quantum well," *Semiconductor science and technology* **23**(12), 125017 (2008).

29 C. J. Ford, "Transporting and manipulating single electrons in surface-acoustic-wave minima," *physica status solidi (b)* **254**(3), 1600658 (2017).

30 P. Batista, M. Gustafsson, M. de Lima Jr, *et al.*, "Acousto-electric single-photon detector," in *Photon Counting Applications, Quantum Optics, and Quantum Cryptography*, **6583**, 36–48, SPIE (2007).

31 P. Batista, R. Hey, and P. Santos, "Efficient electrical detection of ambipolar acoustic transport in gaas," *Applied Physics Letters* **92**(26), 262108 (2008).

32 H. Choi, Y. Nam, J.-H. Lee, *et al.*, "Properties of a surface-gate-controlled two-dimensional electron gas in undoped gaas/algaas heterostructures," *Journal of the Korean Physical Society* **76**(12), 1083–1087 (2020).

33 A. Hernández-Mínguez, M. Møller, S. Breuer, *et al.*, "Acoustically driven photon antibunching in nanowires," *Nano letters* **12**(1), 252–258 (2012).

34 S. Hermelin, S. Takada, M. Yamamoto, *et al.*, "Electrons surfing on a sound wave as a platform for quantum optics with flying electrons," *Nature* **477**(7365), 435–438 (2011).

35 P. Harrison and A. Valavanis, *Quantum wells, wires and dots: theoretical and computational physics of semiconductor nanostructures*, John Wiley & Sons (2016).

36 J. A. Gil-Corrales, J. A. Vinasco, A. Radu, *et al.*, "Self-consistent schrödinger-poisson study of electronic properties of gaas quantum well wires with various cross-sectional shapes," *Nanomaterials* **11**(5), 1219 (2021).

37 H. Hebal, Z. Koziol, S. Lisesivdin, *et al.*, "General-purpose open-source 1d self-consistent schrödinger-poisson solver: Aestimo 1d," *Computational Materials Science* **186**, 110015 (2021).

38 F. Ahlers, N. Fletcher, J. Ebbecke, *et al.*, "Surface acoustic wave driven quantized current transport," *Current Applied Physics* **4**(5), 529–533 (2004).

39 J. S. Ahn, "Finite difference method for the arbitrary potential in two dimensions: Application to double/triple quantum dots," *Superlattices and Microstructures* **65**, 113–123 (2014).

40 T. Bretagnon, P. Lefebvre, P. Valvin, *et al.*, "Radiative lifetime of a single electron-hole pair in GaN/AlN quantum dots," *Phys. Rev. B* **73**, 113304 (2006).

41 Z. Pang, W. Cao, and Y. Bai, "Simulations of the radiative lifetime in surface acoustic wave driven piezoelectric semiconductor devices," in *2022 23rd International Conference on Electronic Packaging Technology (ICEPT)*, 1–5 (2022).

42 C. Wood and D. Jena, *Polarization effects in semiconductors: from ab initio theory to device applications*, Springer Science (2007).

43 H. Gauck, T. Gfroerer, M. Renn, *et al.*, “External radiative quantum efficiency of 96% from a GaAs/GaInP heterostructure,” *Applied Physics A* **64**(2), 143–147 (1997).